Original Article

Absorption spectral study for the interaction of Pr(III) with L-Aspartic acid in various aquated organic solvents through 4f-4f transition spectra: Analysis of reaction pathways and thermodynamic parameters

Juliana Sanchu[1], Chubazenba Imsong[2], Zevivonii Thakro[3], Mhasiriekho Ziekhrü[4], M.I. Devi[5]*

[1,2,3,4,5]Department of Chemistry, Nagaland University; Lumami 798627, India.

Email: cam_indira@yahoo.co.in

DOI: 10.47750/pnr.2022.13.S01.105

Abstract

The interaction of Praseodymium (III) with L-Aspartic Acid has been analysed theoretically through 4f-4f transition in various aquated organic solvents (DMF, ACN, Dioxane and methanol). Spectral parameters such as: Energy interaction parameters like Slater–Condon (Fk's), Lande factor (ξ4f), Racah energy (Ek), nephelauxetic effect (β), bonding (b1/2) and percent covalency (δ), as well as intensity parameters: oscillator strength 'P' and Judd–Ofelt Tλ (λ=2,4,6) were evaluated. The degree of outer and inner sphere coordination, the level of metal 4f-4f orbital involvement in the complexation, defining the immediate coordination environment around the metal Pr(III), and the coordination number of the complex formed could be revealed through the analysis of these spectral parameters. The rate of complexation for Pr(III) with L-Aspartic acid and consequently its thermodynamic parameters have been evaluated through 4f-4f transition spectra.

Keywords: Oscillator strength, Nephelauxetic effect, Amino acids, Pr (III), Coordination number, Thermodynamic parameters.

INTRODUCTION

In recent decades Lanthanide chemistry has received a lot of attention. Lanthanides are used as structural and functional probes to understand biomolecule structures, conformations and properties[1–3]. Many of the concepts and hypotheses have been amended or abandoned as the science of coordination chemistry progresses. Complex formation processes are a "key" in several research fields like analytical, bioinorganic, clinical and biochemical aspects of coordination chemistry has an emerging research area[4][5][6][7].

Under certain experimental and physiological circumstances, lanthanide (III) ions are hard metal ions, preferring hard donor ligands such as oxygen, halogen and nitrogen. In multidentate large biological molecules, there are many ligands containing oxygen, nitrogen, sulphur, halogen and phosphorous donor atoms in the form of functional groups[8]. While analysing the comparison in the absorption spectra of Pr(III): amino acids complex quantitatively, we discovered some interesting structural information about the amino acid molecule, including its coordinating sites[9]. When Pr(III) binds to amino acids, the energies of 4f-4f bands shifts, reducing the energy interaction parameters such as Fk, ξ4f and Ek of 4f-4f electronic transitions[10]. Amino acids contain amine and carboxylic acid functional groups and can modify the form and size of buoyant materials while maintaining the -R group (side chains) [11]. Amino acids are essential to our general health since they play a critical role in enzyme and protein synthesis and contribute significantly to human health, the brain system, hormone secretion and muscle construction. They are also required for the proper functioning of vital cellular and organ networks[12,13]. It has been thoroughly examined how different lanthanides interact with a wide spectrum of proteins, amino acids, and polypeptides [14]. In complexation, lanthanides favour donor atoms in the following order: O>N>S and F>Cl. This indicates that the lanthanide ion has a strong preference for 'O' donor atoms. There is strong evidence of the bonding of Ln (III) ions with amino acids; Ln(III) ion is bonded with the carboxylate group's oxygen atom and the amine group's nitrogen atom [15]. Amino acids exist in a neutral state when they are in the solid phase. As seen in image 1, if their isoelectric point is preserved, they exist as zwitterions in aquated solution. [16]

The inner structure of the lanthanide (III) complex can be revealed by examining the 4f-4f transition spectra. Using 4f-4f transition spectra recorded in various aquated organic solvents, the energy interaction and intensity parameters for the

complexation of Pr (III) with amino acids, other ligands and polypeptides including O, N, and S donors were examined [13–15]. The spectroscopic characteristics of trivalent lanthanide ions are unusual. Because the overlaying 5s2 and 5p6 shells shelter the 4f electrons from external forces, the electron cloud of the Ln (III) ion is mostly unaffected by the ligand environment.[20] The f-f transitions spectra are responsible for the absorption spectra of trivalent lanthanide ions. As a result, the absorption spectra of lanthanide complexes are often sharp and line-like, in contrast to transition metal's broad absorption bands. The f-f bands' intensity is affected by the nature of the coordination sphere in a quantitative way [21].

Comparative absorption spectroscopy was used in this study to estimate the energy interaction and intensity parameters for the complexation of praseodymium (III) with L-aspartic acid in various aqueous organic solvents. The fluctuation in spectral characteristics could reveal the mechanism of binding in terms of inner and outer-sphere complexation, degree of covalency, and 4f-orbital involvement. The simultaneous coordination of Pr(III): L-Aspartic acid complex at various temperatures in DMF medium was investigated using reaction rate and thermodynamic parameters to investigate reaction rate, pre-exponential factors, and thermodynamic parameters.

Materials and methods:

Praseodymium (III) chloride hydrate was purchased from Sigma Aldrich with 99.9% purity, and L-Aspartic acid from HIMEDIA are used for spectral and kinetic studies. The solvents used DMF, ACN, Dioxane and MeOH are of A/R grade from E. Merck. The concentrations of Pr(III):L-Aspartic acid complex were kept at 0.01 M and the pH was maintained to 2.77. In all the preparations, binary mixtures (50%v/v) of water in four different organic solvents (Acetonitrile, Dioxane, Dimethylformamide & Methanol) were used. The absorption spectra were recorded using a UV-Vis spectrophotometer (Perkin Elmer Lambda 365).

For kinetic experiments, equimolar quantities of Pr(III):L-Aspartic acid complex was added to aquated DMF solvent and the resulting mixture was agitated in an inert atmosphere generated to form the complex in solution. All spectra were taken using a Perkin Elmer Lambda-35 UV-Visible Spectrophotometer with a connected kinetic assembly that was temperature-controlled. Water flowing HAAKE DC 10 thermostat is used to maintain the desired temperature.

Praseodymium (III) with Amino acids form Metal Complex

Praseodymium (III) are "hard acids" and hard acceptors, they prefer to form complexes with "hard bases" and hard donor ligands. Coordination numbers typically range from 6 to 12, the physiologically significant being 8 or 9. Therefore, the complexes can take on a variety of geometrical forms. In their solid-state, amino acids are neutral. However, when they are dissolved in an aqueous medium and their isoelectric point is maintained, they exist as zwitterions as shown in figure 1 [22–24].

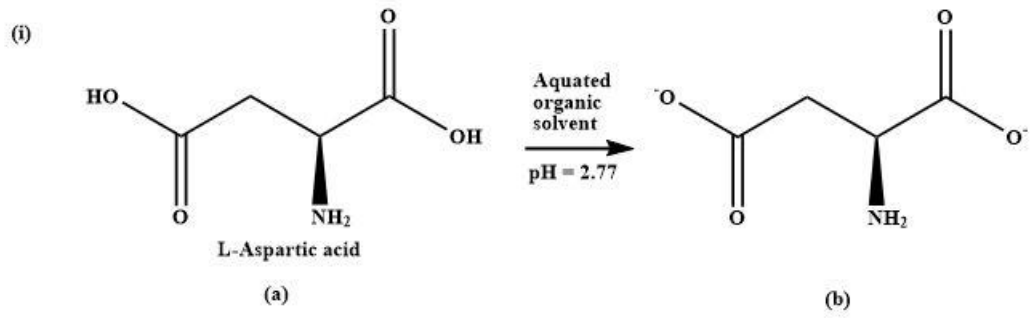

Figure 1: The zwitterions of L-Aspartic acid.

When the value of the pH is less than 7, only the ‘O’ atom bind to the metal ion; but when the pH value is above 7, both ‘O’ atom and ‘N’ atom bind with the metal ion [25]. Since the isoelectric point of L-aspartic acid is pH 2.77 the metal ion interacts with only the oxygen atoms of the L-Aspartic acid and acts as bidentate, forming a complex with the praseodymium(III) as given in figure 2.

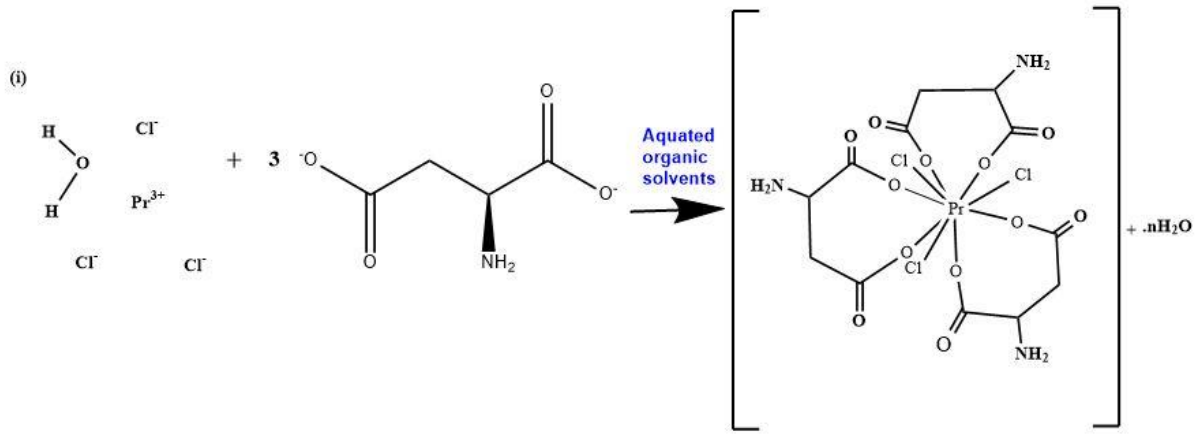

Figure 2: Chemical reaction pathway of Praseodymiuym(III) with L-Aspartic acid complex in aquated medium

Theoretical

Energy parameters

The Nephelauxetic ratio is determined by the covalency, as illustrated below.

$$\beta = \frac{F_K^C}{F_K^f} \text{ or } \frac{E_C^K}{E_f^K}$$

For complex and free ions, Slater–Condon parameters are written as FK while Racah parameters are expressed as EK. Covalent percentage and bonding parameter are calculated using the equations given below;

$$b^{1/2} = \left[\frac{1-\beta}{2}\right]^{1/2}$$

$$\delta = \left[\frac{1-\beta}{\beta}\right] \times 100$$

The Electrostatic term E0 was stated as, using the Slater radial integral and the Slater-Condon parameter.

$$E_0 = \sum_{k=0}^{k=6} K^k F_k$$

Where K^k is the angular coefficient.

The direct-integrals, or Slater-Condon parameters (Fk), are a decreasing function of K with the relationship given as,

$$F_1^k = \int_0^\infty \int_0^\infty \frac{r_<^k}{r_>^{k=1}} R_i^2(r_i) R_j^2(r_j) r_i^2 r_j^2 dr_i dr_j$$

The near and distant electron radii are 'r_< & r_>', the 4f-radial wave function is 'R,' and the ith & jth electrons are 'i & j'. Condon and Shortley reformulated the Slater-Condon parameter (Fk) integrals in terms of reduced integrals (Fk).

$$F_k = \frac{F^k}{D_k}$$

Combining the above two relations, the reduced Slater-Condon integral is given by an equation,

$$F_k = \frac{1}{D_k} \int_0^\infty \int_0^\infty \frac{r_<^k}{r_>^{k=1}} R_i^2(r_i) R_j^2(r_j) r_i^2 r_j^2 dr_i dr_j$$

The linear combinations of F_k are given as the energy interaction parameter Racah E^ki,

$$E^1 = \frac{70F_2 + 231F_4 + 20.02F_6}{9}$$

$$E^2 = \frac{F_2 - 3F_4 + 7F_6}{9}$$

$$E^3 = \frac{5F_2 + 6F_4 - 9F_6}{3}$$

The energy (Eso) in 4f–4f electronic transition is known to come from a significant magnetic contact, but the spin-orbit interactions may be written as,

$$E_{so} = A_{so}\ \xi_{4f}$$

where 'ξ4f' denotes the radial integral and 'Aso' denotes the angular component of spin-orbit interaction. By first-order approximation, the energy Ej of the jth level is represented as,

$$E_j(F_k, \xi_{4f}) = E_{oj}(F_k^0, \xi_{4f}) + \frac{\partial E_j}{\partial F_k}\Delta F_K + \frac{\partial E_j}{\partial \xi 4f}\Delta\ \xi_{4f}$$

where 'E0j' denotes the jth level's zero-order energy. The equivalent values of FK and ξ4f are provided in the equations below.

$$F_k = F_k^0 + \Delta F_k$$

$$\xi_{4f} = \xi_{4f}^0 + \Delta\xi_{4f}$$

The zero-order ΔEj and the observed value of Ej are expressed by the given equation,

$$\Delta E_j = \sum_{k\ 2,4,6} \frac{\partial E_j}{\partial F_K} + \frac{\partial E_j}{\partial \xi_{4f}}\Delta\xi_{4f}$$

The following problem may be solved using the least square approach to determine the values of ΔF_2 & $\Delta\xi_{4f}$.

The following is the formula for determining the estimated values of F_4 and F_6:

$$\frac{F_4}{F_2} = 0.1380\ and\ \frac{F_6}{F_2} = 0.0150$$

Intensity Parameters

Judd[26] and Ofelt[27] established a theoretical technique for calculating band intensities. They thought the transitions are essentially electric dipole transitions, and that the oscillator strength corresponding to the induced electric dipole transition ΨJ → Ψ/J/ as given by

$$\sum_{\lambda=2,4,6} T_\lambda \sigma(f^N\ \psi\ J \| U^{\lambda\lambda} \| f^N \psi'\ J')^2 \ldots\ldots\ldots\ldots\ldots\ldots\ldots\ldots\ (1)$$

The rank matrix element is denoted by U(λ). The three numbers T2, T4, and T6 are associated with the radial components of the 4fN wave functions, the closest of which is 4fN-15d.

The expression connects the measured intensity of an absorption band to the probability (P) of radiant energy absorption (oscillator strength):

$$P = \frac{2303mc^2}{N\pi e^2}\int \varepsilon_i\,(\sigma)d\sigma$$

$$P = 4.318 \times 10^{-9} \int \varepsilon_i\,(\sigma)d\sigma \ldots\ldots\ldots\ldots\ldots\ldots\ldots\ldots\ldots\ldots\ldots\ldots\ (2)$$

The intensity of the absorption band is determined by the experimentally observed oscillator strength (Pobs), which is directly proportional to the area under the absorption curve and is estimated using Gaussian curve analysis:

$$P = 4.60 \times 10^{-9} \times \varepsilon_{max} \times \Delta v_{\frac{1}{2}} \ldots\ldots\ldots\ldots\ldots\ldots\ldots\ldots\ldots\ldots\ldots\ldots\ldots \quad (3)$$

The molar extinction coefficient is given by εmax.

The T2, T4 and T6 values supplied by Judd and Ofelt were utilised to represent the computed oscillator strength (Pobs) of the transition energies, as derived by the equation below.

$$\frac{P_{obs}}{v} = [(U^2)]^2T_2 + [(U^4)]^2T_4 + [(U^6)]^2T_6 \ldots\ldots\ldots\ldots\ldots\ldots\ldots\ldots\ldots \quad (4)$$

Carnall[26] gave the matrix elements of Pr(III) system as U(λ).

Rate of the reactions

Based on the concept of activation energy. Arrhenius described the temperature dependence of the rate constant (k) by the equation,

$$k = Ae^{\frac{-E_a}{RT}} \ldots\ldots\ldots\ldots\ldots\ldots\ldots\ldots\ldots\ldots\ldots \quad (5)$$

This equation is known as the Arrhenius rate equation.

Where A stands for frequency factor. The factor exp (-Ea/RT) is a measure of the likelihood of a molecule being in an activated state.

Plotting graph log k (rate constant) versus 1/T yields the Arrhenius rate equation, which is used to determine the activation energy for the Pr(III):L-Aspartic acid complex in DMF solvent. [29,30]

The equation (5) may be expressed as follows:

$$\ln k = \ln A - \frac{E_a}{RT}$$

$$\text{or, } 2.303\log k = 2.303\log A - \frac{E_a}{RT}$$

$$\text{or, } \log k = \log A - \frac{E_a}{2.303RT} \quad \ldots\ldots\ldots\ldots\ldots\ldots \quad (6)$$

where, A = pre-exponential factor, often known as the frequency factor.

As a result, plotting log k versus 1/T should provide a straight line with a negative slope.

$$\text{Slope} = \frac{E_a}{2.303R} \quad \text{and Intercept} = \log A$$

The activation energy Ea is calculated from the slope as

$$E_a = -\text{Slope} \times 2.303 \times R \ldots\ldots\ldots\ldots\ldots\ldots\ldots\ldots\ldots\ldots\ldots\ldots\ldots \quad (7)$$

Where R is the universal gas constant

The complexation's thermodynamic characteristics were established using a Van't Hoff plot of log k versus 1/T×10^3, which was provided as

$$\log k = -\frac{\Delta H^\circ}{R}\left[\frac{1}{T}\right] + \frac{\Delta S^\circ}{R} \ldots\ldots\ldots\ldots\ldots\ldots\ldots\ldots\ldots\ldots\ldots\ldots\ldots\ldots \quad (8)$$

$$\text{Or } \log k = -\frac{\Delta G^\circ}{RT}$$

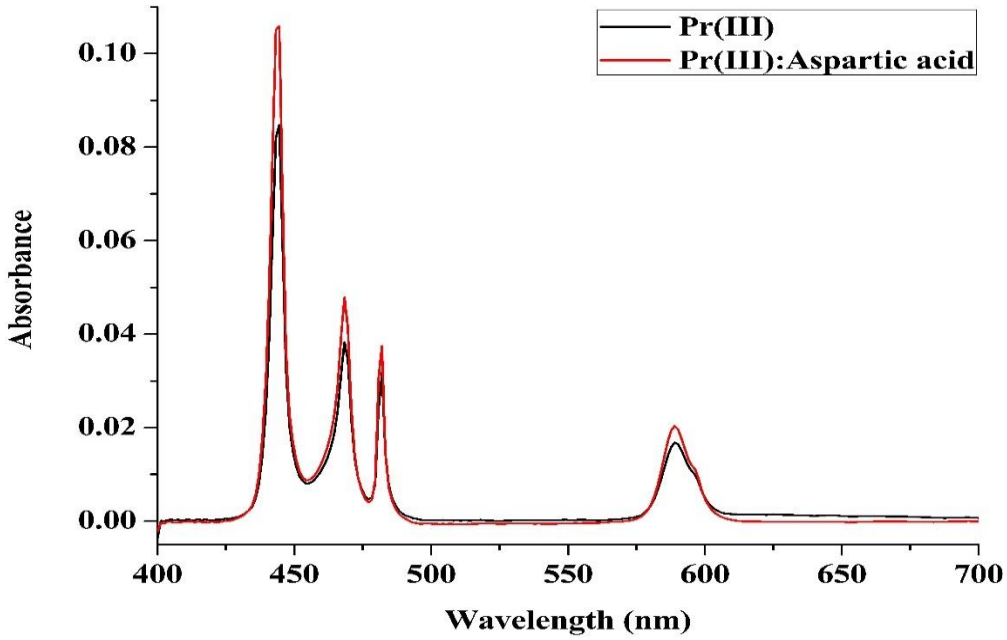

Figure 3: UV-vis spectra of Praseodymium(III) and Praseodymium(III):L-Aspartic acid complex in aquated DMF solvent.

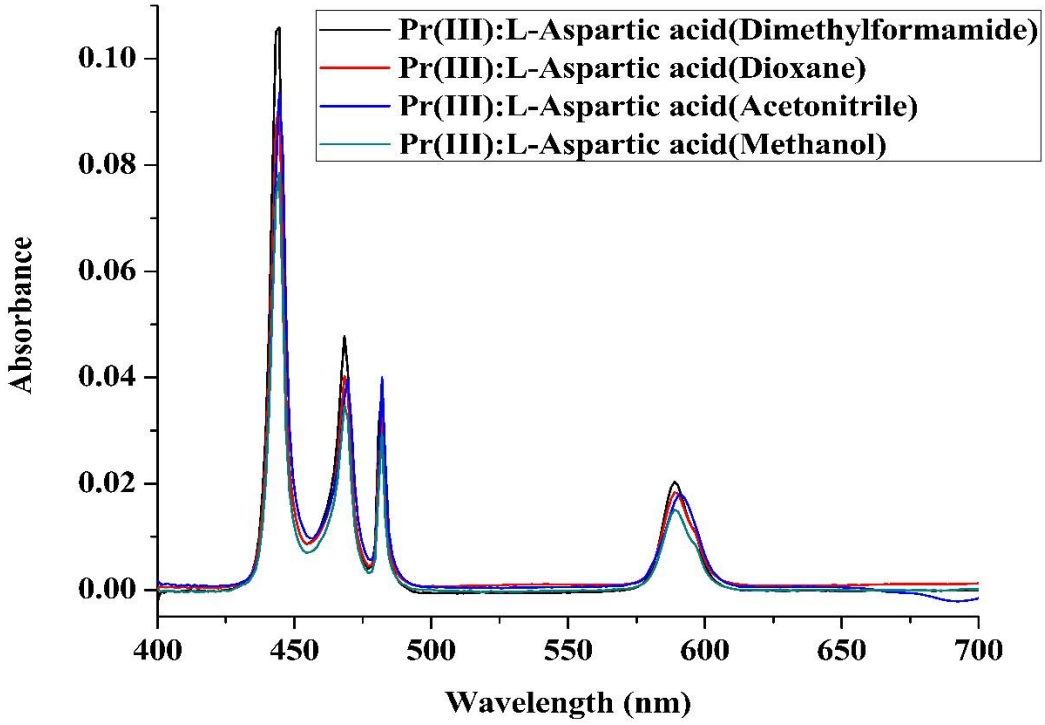

Figure 4: UV-vis absorption spectra of Praseodymium(III):L-Aspartic acid complex in various aquated organic solvents.

Table 1. Comparative studies of energy interaction values- Slater–Condon (Fk), Lande (ξ4f), Racah energy (Ek), Nephelauxetic ratio (β), bonding (b1/2), and covalency (δ) factors of Praseodymium(III) and Praseodymium(III):L-Aspartic acid complex in various aqueous medium

Systems	F_2	F_4	F_6	ξ_{4f}	E^1	E^2	E^3	β	$b^{1/2}$	δ
ACETONITRILE										
Pr(III)	**309.523**	**44.534**	**6.691**	**724.72**	**3612.55**	**25.327**	**589.34**	**0.947**	**0.1616**	**5.612**
Pr(III)+Aspartic Acid	**309.294**	**44.512**	**6.672**	**724.49**	**3612.34**	**25.311**	**588.96**	**0.948**	**0.1628**	**5.634**
DIMETHYLFORMAMIDE										
Pr(III)	**309.043**	**44.572**	**6.759**	**725.33**	**3613.21**	**25.376**	**589.78**	**0.946**	**0.1631**	**5.703**
Pr(III)+Aspartic Acid	**309.020**	**44.537**	**6.731**	**724.94**	**3612.92**	**25.298**	**589.34**	**0.949**	**0.1642**	**5.741**
1,4-DIOXANE										
Pr(III)	**309.196**	**44.493**	**6.654**	**724.52**	**3612.32**	**25.318**	**589.21**	**0.947**	**0.1609**	**5.609**
Pr(III)+Aspartic Acid	**309.173**	**44.469**	**6.633**	**724.25**	**3612.15**	**25.294**	**588.83**	**0.948**	**0.1619**	**5.627**
METHANOL										
Pr(III)	**309.323**	**44.474**	**6.639**	**724.48**	**3612.09**	**25.274**	**589.05**	**0.945**	**0.1589**	**5.594**
Pr(III)+Aspartic Acid	**309.305**	**44.427**	**6.613**	**724.12**	**3611.85**	**25.248**	**588.77**	**0.947**	**0.1611**	**5.621**

Table 2. Comparative studies of energies (cm−1) values as well as RMS values for Praseodymium(III) and Praseodymium(III):L-Aspartic acid in various aqueous medium.

Systems	$^3H_4 \rightarrow {}^3P_2$		$^3H_4 \rightarrow {}^3P_1$		$^3H_4 \rightarrow {}^3P_0$		$^3H_4 \rightarrow {}^1D_2$		RMS
	E_{obs}	E_{cal}	E_{obs}	E_{cal}	E_{obs}	E_{cal}	E_{obs}	E_{cal}	
ACETONITRILE									
Pr(III)	**22626.84**	**22543.21**	**22247.33**	**22185.47**	**21763.55**	**21649.72**	**18945.34**	**19146.05**	**102.56**

Pr(III)+ Aspartic Acid	**22626.63**	**22527.66**	**22229.14**	**22170.89**	**21741.29**	**21621.43**	**18925.11**	**19120.52**	**102.33**
DIMETHYLFORMAMIDE									
Pr(III)	**22627.13**	**22575.31**	**22273.67**	**22199.15**	**21789.23**	**21689.43**	**18968.61**	**19178.63**	**102.81**
Pr(III)+ Aspartic Acid	**22626.63**	**22556.63**	**22251.61**	**22183.09**	**21763.75**	**21643.09**	**18947.07**	**19151.23**	**102.46**
1,4-DIOXANE									
Pr(III)	**22626.72**	**22529.71**	**22231.09**	**22152.76**	**21736.43**	**21626.21**	**18923.14**	**19125.72**	**102.32**
Pr(III)+ Aspartic Acid	**22626.51**	**22505.37**	**22213.65**	**22129.41**	**21717.79**	**21603.76**	**18901.51**	**19101.34**	**102.12**
METHANOL									
Pr(III)	**22626.69**	**22513.58**	**22207.82**	**22135.72**	**21719.65**	**21638.26**	**18921.56**	**19104.62**	**102.14**
Pr(III)+ Aspartic Acid	**22626.39**	**22498.27**	**22185.62**	**22094.56**	**21689.23**	**21612.87**	**18889.23**	**19092.13**	**102.05**

Table 3. Comparative studies of Oscillator strengths and Judd–Ofelt parameters for Praseodymium(III) and Praseodymium(III):L-Aspartic acid complex in various aqueous medium.

Systems	**$^3H_4 \rightarrow {}^3P_2$**		**$^3H_4 \rightarrow {}^3P_1$**		**$^3H_4 \rightarrow {}^3P_0$**		**$^3H_4 \rightarrow {}^1D_2$**		**T_2**	**T_4**	**T_6**
	Pobs	**Pcal**	**Pobs**	**Pcal**	**Pobs**	**Pcal**	**Pobs**	**Pcal**			
ACETONITRILE											
Pr(III)	**17.265**	**17.265**	**5.321**	**4.428**	**2.265**	**3.067**	**2.197**	**2.197**	**-253.2**	**10.127**	**54.321**
Pr(III)+Aspartic Acid	**21.735**	**21.735**	**5.721**	**4.699**	**3.595**	**4.321**	**3.765**	**3.765**	**-350.4**	**11.893**	**67.853**
DIMETHYLFORMAMIDE											
Pr(III)	**19.042**	**19.042**	**5.542**	**4.456**	**2.367**	**4.256**	**3.623**	**3.623**	**-321.7**	**12.153**	**53.428**
Pr(III)+Aspartic Acid	**20.098**	**20.098**	**5.921**	**4.761**	**2.972**	**4.541**	**4.035**	**4.035**	**-465.1**	**13.239**	**62.653**
1,4- DIOXANE											

Pr(III)	**17.623**	**17.623**	**5.278**	**4.165**	**2.231**	**3.967**	**2.978**	**2.978**	**-209.5**	**10.078**	**49.152**
Pr(III)+Aspartic Acid	**19.326**	**19.326**	**5.567**	**4.539**	**3.389**	**4.349**	**3.436**	**3.436**	**-312.9**	**12.217**	**55.294**
METHANOL											
Pr(III)	**15.723**	**15.723**	**5.123**	**4.067**	**1.725**	**3.721**	**2.749**	**2.749**	**-189.3**	**10.026**	**52.236**
Pr(III)+Aspartic Acid	**17.265**	**17.265**	**5.434**	**4.478**	**2.328**	**4.167**	**2.967**	**2.967**	**-232.5**	**12.518**	**57.447**

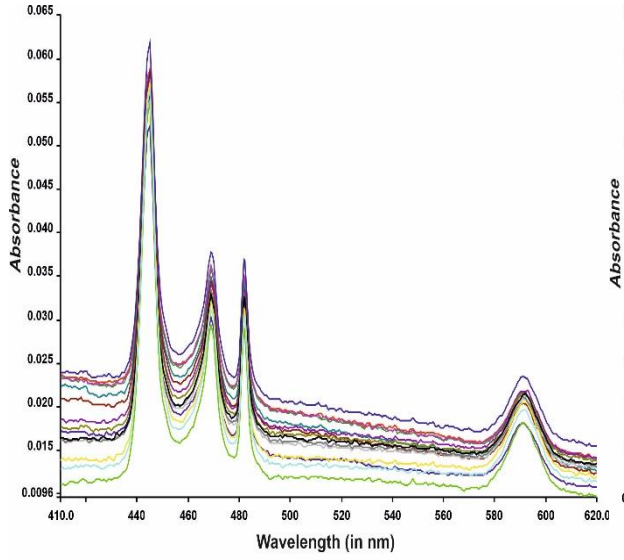

Absorption spectra of Pr(III):L-Aspartic acid complexation at different hours at 298K (25°C)

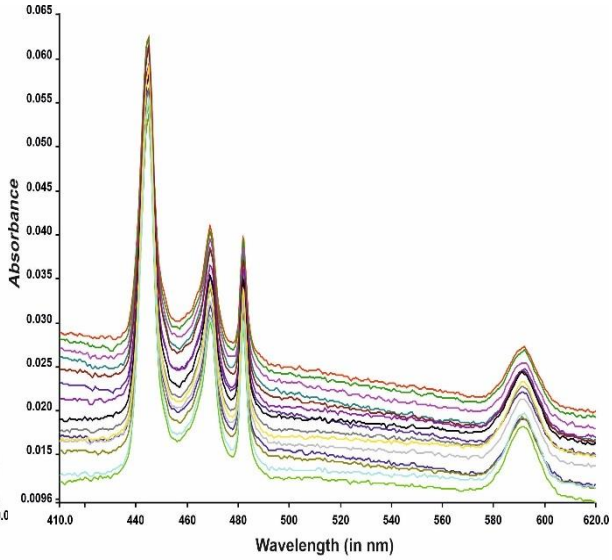

Absorption spectra of Pr(III):L-Aspartic acid complexation at different hours at 303K (30°C)

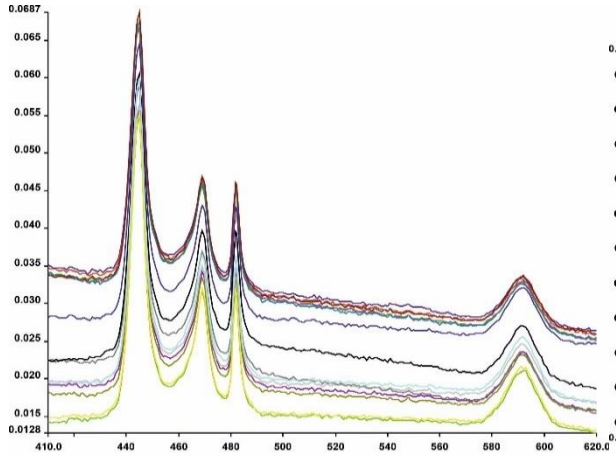

Absorption spectra of Pr(III):L-Aspartic acid complexation at different hours at 308K (35°C)

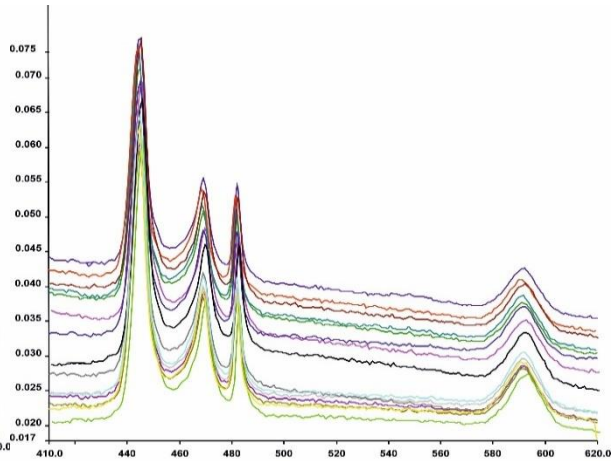

Absorption spectra of Pr(III):L-Aspartic acid complexation at different hours at 313K (40°C)

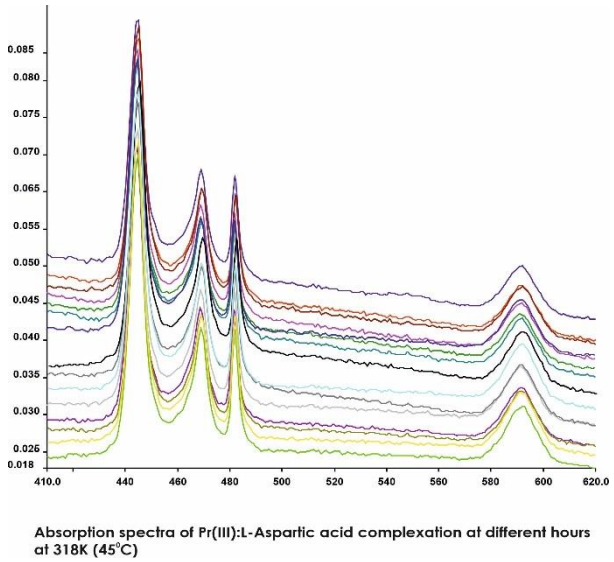

Figure 5: Absorption spectrum for Praseodymium (III): L-Aspartic acid complex in DMF medium at different time intervals of 25°C, 30°C, 35°C, 40°C and 45°C

Table 4: Oscillator Strengths and Judd-Ofelt parameters for Praseodymium(III):L-Aspartic acid complex at different time intervals of 298 K(25°C)

System	$^3H_4 \rightarrow {}^3P_2$		$^3H_4 \rightarrow {}^3P_1$		$^3H_4 \rightarrow {}^3P_0$		$^3H_4 \rightarrow {}^1D_2$		T_2	T_4	T_6
	P_{obs}	P_{cal}	P_{obs}	P_{cal}	P_{obs}	P_{cal}	P_{obs}	P_{cal}			
0	4.711	4.711	2.612	1.865	1.181	1.911	1.804	1.804	79.023	4.187	14.460
2	4.921	4.921	2.623	1.932	1.234	1.894	1.775	1.775	79.245	4.398	14.945
4	5.131	5.131	2.645	1.966	1.265	1.933	1.815	1.815	81.923	4.821	15.332
6	5.223	5.223	2.665	1.992	1.279	1.967	1.921	1.921	88.921	4.943	15.873
8	5.407	5.407	2.763	2.067	1.355	2.036	2.113	2.113	91.231	5.466	16.231
10	5.545	5.545	2.846	2.097	1.367	2.099	2.267	2.267	171.431	5.687	16.436
12	5.672	5.672	2.883	2.133	1.396	2.128	2.345	2.345	202.321	5.977	16.643
14	5.723	5.723	2.925	2.185	1.411	2.165	2.431	2.431	208.562	6.056	16.851
16	5.851	5.851	2.966	2.212	1.485	2.197	2.546	2.546	210.214	6.167	18.176
18	5.915	5.915	3.038	2.279	1.513	2.265	2.672	2.672	211.875	6.269	18.598
20	6.149	6.149	3.125	2.334	1.554	2.329	2.754	2.754	270.137	6.559	18.784
22	6.246	6.246	3.236	2.451	1.620	2.435	2.918	2.918	273.751	6.749	18.904
24	6.355	6.355	3.376	2.545	1.767	2.523	3.075	3.075	276.920	6.921	19.123
26	6.429	6.429	3.534	2.631	1.823	2.646	3.156	3.156	285.706	7.063	19.334
28	6.541	6.541	3.625	2.756	1.891	2.727	3.227	3.227	308.334	7.137	19.525
30	6.653	6.653	3.768	2.867	1.908	2.816	3.454	3.454	345.413	7.285	19.667
32	6.718	6.718	3.838	2.952	1.976	2.881	3.523	3.523	359.202	7.564	19.843

34	**6.823**	**6.823**	**3.974**	**3.066**	**2.026**	**2.935**	**3.741**	**3.741**	**401.576**	**7.758**	**20.266**

Table 5: Oscillator Strengths and Judd-Ofelt parameters for Praseodymium(III):L-Aspartic acid complex at different time intervals of 303 K(30°C)

System	$^3H_4 \rightarrow {}^3P_2$		$^3H_4 \rightarrow {}^3P_1$		$^3H_4 \rightarrow {}^3P_0$		$^3H_4 \rightarrow {}^1D_2$		T_2	T_4	T_6
	P_{obs}	P_{cal}	P_{obs}	P_{cal}	P_{obs}	P_{cal}	P_{obs}	P_{cal}			
0	**5.523**	**5.523**	**1.195**	**1.079**	**1.075**	**1.091**	**1.342**	**1.342**	**215.230**	**3.731**	**17.845**
2	**5.756**	**5.756**	**1.366**	**1.147**	**1.091**	**2.046**	**1.557**	**1.557**	**204.312**	**4.145**	**19.361**
4	**5.921**	**5.921**	**3.154**	**2.187**	**1.165**	**2.147**	**1.107**	**1.107**	**187.542**	**5.817**	**20.056**
6	**6.156**	**6.156**	**3.232**	**2.247**	**1.223**	**2.246**	**1.168**	**1.168**	**175.527**	**6.231**	**20.189**
8	**6.325**	**6.325**	**2.756**	**1.985**	**1.241**	**1.953**	**1.227**	**1.227**	**163.606**	**5.326**	**20.556**
10	**6.562**	**6.562**	**2.768**	**2.023**	**1.263**	**1.995**	**1.338**	**1.338**	**149.805**	**5.535**	**20.609**
12	**6.735**	**6.735**	**2.742**	**2.071**	**1.304**	**2.007**	**1.447**	**1.447**	**137.163**	**5.656**	**20.665**
14	**6.967**	**6.967**	**2.797**	**2.056**	**1.389**	**2.114**	**1.545**	**1.545**	**140.427**	**5.723**	**21.314**
16	**7.008**	**7.008**	**3.121**	**2.265**	**1.411**	**2.239**	**1.768**	**1.768**	**133.712**	**6.217**	**21.452**
18	**7.167**	**7.167**	**3.245**	**2.361**	**1.447**	**2.341**	**1.969**	**1.969**	**36.274**	**6.467**	**21.942**
20	**7.245**	**7.245**	**3.411**	**2.439**	**1.502**	**2.412**	**2.073**	**2.073**	**16.434**	**6.752**	**22.324**
22	**7.573**	**7.573**	**3.485**	**2.531**	**1.585**	**2.491**	**2.139**	**2.139**	**21.507**	**6.959**	**22.954**
24	**7.761**	**7.761**	**3.513**	**2.572**	**1.614**	**2.522**	**2.371**	**2.371**	**9.318**	**7.043**	**23.125**
26	**7.827**	**7.827**	**3.647**	**2.663**	**1.659**	**2.607**	**2.463**	**2.463**	**45.164**	**7.353**	**23.641**
28	**7.914**	**7.914**	**3.721**	**2.725**	**1.692**	**2.675**	**2.529**	**2.529**	**58.173**	**7.463**	**23.743**
30	**8.168**	**8.168**	**4.429**	**3.086**	**1.714**	**3.146**	**2.783**	**2.783**	**65.239**	**8.556**	**25.068**
32	**8.382**	**8.382**	**5.047**	**3.371**	**1.783**	**3.447**	**2.912**	**2.912**	**66.428**	**9.571**	**25.487**
34	**8.582**	**8.582**	**3.634**	**2.962**	**1.828**	**2.849**	**3.065**	**3.065**	**121.135**	**7.917**	**25.891**

Table 6: Oscillator Strengths and Judd-Ofelt parameters for Praseodymium(III):L-Aspartic acid complex at different time intervals of 308 K(35° C)

System	$^3H_4 \rightarrow {}^3P_2$		$^3H_4 \rightarrow {}^3P_1$		$^3H_4 \rightarrow {}^3P_0$		$^3H_4 \rightarrow {}^1D_2$		T_2	T_4	T_6
	P_{obs}	P_{cal}	P_{obs}	P_{cal}	P_{obs}	P_{cal}	P_{obs}	P_{cal}			
0	**6.521**	**6.521**	**2.635**	**1.711**	**0.646**	**1.669**	**1.121**	**1.121**	**78.145**	**4.643**	**20.421**
2	**6.643**	**6.643**	**2.741**	**1.823**	**0.723**	**1.729**	**1.357**	**1.357**	**78.341**	**4.862**	**20.569**
4	**6.755**	**6.755**	**2.852**	**1.936**	**0.845**	**1.841**	**1.573**	**1.573**	**66.705**	**5.497**	**20.656**
6	**6.813**	**6.813**	**2.942**	**2.008**	**0.898**	**1.967**	**1.636**	**1.636**	**76.187**	**5.775**	**20.832**

8	**6.962**	**6.962**	**3.017**	**2.145**	**0.904**	**2.085**	**1.742**	**1.742**	**38.428**	**5.887**	**21.362**
10	**7.039**	**7.039**	**3.165**	**2.263**	**0.947**	**2.138**	**1.838**	**1.838**	**42.276**	**5.945**	**21.672**
12	**7.183**	**7.183**	**3.273**	**2.352**	**0.993**	**2.253**	**1.916**	**1.916**	**44.456**	**5.997**	**22.019**
14	**7.234**	**7.234**	**3.361**	**2.476**	**1.006**	**2.321**	**2.058**	**2.058**	**40.745**	**6.019**	**22.345**
16	**7.341**	**7.341**	**3.446**	**2.531**	**1.018**	**2.392**	**2.148**	**2.148**	**132.415**	**6.096**	**22.567**
18	**7.475**	**7.475**	**3.573**	**2.619**	**1.038**	**2.425**	**2.363**	**2.363**	**37.543**	**6.287**	**22.876**
20	**7.681**	**7.681**	**3.690**	**2.755**	**1.092**	**2.489**	**2.481**	**2.481**	**47.458**	**6.372**	**23.471**
22	**7.767**	**7.767**	**3.756**	**2.838**	**1.114**	**2.556**	**2.546**	**2.546**	**66.371**	**6.463**	**23.535**
24	**7.943**	**7.943**	**3.829**	**2.953**	**1.146**	**2.678**	**2.661**	**2.661**	**48.169**	**6.548**	**24.323**
26	**8.006**	**8.006**	**3.992**	**3.009**	**1.192**	**2.742**	**2.734**	**2.734**	**66.321**	**6.749**	**24.573**
28	**8.216**	**8.216**	**4.051**	**3.156**	**1.236**	**2.837**	**2.826**	**2.826**	**86.538**	**6.992**	**24.729**
30	**8.473**	**8.473**	**4.193**	**3.231**	**1.288**	**2.907**	**2.969**	**2.969**	**91.376**	**7.418**	**25.468**
32	**8.567**	**8.567**	**4.258**	**3.312**	**1.316**	**2.989**	**3.013**	**3.013**	**100.464**	**7.587**	**26.352**
34	**8.748**	**8.748**	**4.385**	**3.476**	**1.371**	**3.069**	**3.145**	**3.145**	**99.276**	**7.276**	**26.867**

Table 7: Oscillator Strengths and Judd-Ofelt parameters for Praseodymium(III):L-Aspartic acid complex at different time intervals of 313 K(40° C)

System	**$^3H_4 \rightarrow {}^3P_2$**		**$^3H_4 \rightarrow {}^3P_1$**		**$^3H_4 \rightarrow {}^3P_0$**		**$^3H_4 \rightarrow {}^1D_2$**		**T_2**	**T_4**	**T_6**
	P_{obs}	**P_{cal}**	**P_{obs}**	**P_{cal}**	**P_{obs}**	**P_{cal}**	**P_{obs}**	**P_{cal}**			
0	**6.532**	**6.532**	**1.812**	**1.623**	**1.417**	**1.623**	**2.645**	**2.645**	**212.561**	**4.537**	**20.175**
2	**6.641**	**6.641**	**1.983**	**1.836**	**1.631**	**1.743**	**2.734**	**2.734**	**234.323**	**5.117**	**20.365**
4	**6.867**	**6.867**	**2.043**	**1.917**	**1.678**	**1.865**	**2.846**	**2.846**	**251.635**	**5.350**	**20.735**
6	**7.037**	**7.037**	**2.174**	**1.987**	**1.708**	**1.956**	**2.951**	**2.951**	**269.266**	**5.832**	**21.537**
8	**7.321**	**7.321**	**2.231**	**2.061**	**1.783**	**2.043**	**3.067**	**3.067**	**263.437**	**5.543**	**22.482**
10	**7.549**	**7.549**	**2.452**	**2.136**	**1.882**	**2.159**	**3.134**	**3.134**	**266.431**	**5.752**	**23.368**
12	**7.811**	**7.811**	**2.531**	**2.251**	**1.955**	**2.238**	**3.265**	**3.365**	**45.672**	**7.291**	**23.653**
14	**7.949**	**7.949**	**2.672**	**2.304**	**1.998**	**2.376**	**3.347**	**3.347**	**243.435**	**5.652**	**24.434**
16	**8.098**	**8.098**	**2.708**	**2.443**	**2.008**	**2.436**	**3.409**	**3.409**	**66.134**	**6.653**	**24.842**
18	**8.213**	**8.213**	**2.785**	**2.567**	**2.089**	**2.498**	**3.574**	**3.574**	**270.456**	**6.762**	**25.365**
20	**8.423**	**8.423**	**4.084**	**2.647**	**2.134**	**2.505**	**3.623**	**3.623**	**91.532**	**7.456**	**25.473**
22	**8.565**	**8.565**	**2.659**	**2.721**	**2.235**	**2.596**	**3.745**	**3.745**	**274.382**	**6.631**	**26.267**
24	**8.677**	**8.677**	**2.934**	**2.836**	**2.341**	**2.625**	**3.813**	**3.813**	**315.438**	**7.264**	**26.453**

26	**8.746**	**8.746**	**3.521**	**2.905**	**2.393**	**2.677**	**3.885**	**3.885**	**209.367**	**6.266**	**26.854**
28	**8.828**	**8.828**	**4.347**	**3.006**	**2.427**	**2.712**	**3.957**	**3.957**	**99.587**	**7.743**	**26.987**
30	**9.453**	**9.453**	**2.173**	**3.113**	**2.481**	**2.747**	**4.007**	**4.007**	**299.683**	**4.365**	**29.765**
32	**9.669**	**9.669**	**3.856**	**3.248**	**2.512**	**2.793**	**4.083**	**4.083**	**151.374**	**7.632**	**29.987**
34	**10.056**	**10.056**	**2.867**	**3.355**	**2.678**	**2.853**	**4.169**	**4.169**	**258.467**	**7.462**	**30.644**

Table 8: Oscillator Strengths and Judd-Ofelt parameters for Praseodymium(III):L-Aspartic acid complex at different time intervals of 318 K(45°C)

System	**$^3H_4 \rightarrow {}^3P_2$**		**$^3H_4 \rightarrow {}^3P_1$**		**$^3H_4 \rightarrow {}^3P_0$**		**$^3H_4 \rightarrow {}^1D_2$**		**T_2**	**T_4**	**T_6**
	P_{obs}	**P_{cal}**	**P_{obs}**	**P_{cal}**	**P_{obs}**	**P_{cal}**	**P_{obs}**	**P_{cal}**			
0	**6.762**	**6.762**	**1.991**	**1.782**	**1.543**	**1.786**	**2.856**	**2.856**	**203.541**	**4.865**	**20.376**
2	**6.945**	**6.945**	**2.045**	**1.866**	**1.649**	**1.856**	**2.967**	**2.967**	**209.633**	**5.345**	**20.554**
4	**7.067**	**7.067**	**2.168**	**1.953**	**1.716**	**1.941**	**3.039**	**3.039**	**261.458**	**5.549**	**20.941**
6	**7.231**	**7.231**	**2.227**	**2.047**	**1.789**	**2.019**	**3.155**	**3.155**	**271.413**	**5.654**	**21.482**
8	**7.459**	**7.459**	**2.356**	**2.231**	**1.852**	**2.123**	**3.226**	**3.226**	**265.827**	**5.861**	**22.630**
10	**7.676**	**7.676**	**2.473**	**2.436**	**1.940**	**2.185**	**3.346**	**3.346**	**268.623**	**6.068**	**23.342**
12	**7.864**	**7.864**	**2.540**	**2.673**	**2.017**	**2.234**	**2.461**	**2.461**	**48.719**	**6.361**	**23.558**
14	**8.057**	**8.087**	**2.607**	**2.721**	**2.069**	**2.387**	**3.589**	**3.589**	**246.347**	**6.543**	**24.376**
16	**8.253**	**8.253**	**2.745**	**2.789**	**2.178**	**2.453**	**3.664**	**3.664**	**69.381**	**6.843**	**24.896**
18	**8.491**	**8.491**	**2.952**	**2.824**	**2.221**	**2.584**	**3.721**	**3.721**	**273.425**	**6.952**	**25.469**
20	**8.653**	**8.653**	**3.084**	**2.876**	**2.294**	**2.638**	**3.855**	**3.855**	**94.456**	**7.267**	**25.921**
22	**8.844**	**8.844**	**3.254**	**2.921**	**2.356**	**2.679**	**3.954**	**3.954**	**278.309**	**7.459**	**26.256**
24	**8.912**	**8.912**	**3.476**	**2.992**	**2.432**	**2.745**	**3.989**	**3.989**	**317.417**	**7.660**	**26.864**
26	**9.058**	**9.058**	**3.753**	**3.043**	**2.491**	**2.809**	**2.345**	**2.345**	**212.367**	**7.857**	**27.658**
28	**9.475**	**9.475**	**3.905**	**3.127**	**2.523**	**2.876**	**4.019**	**4.019**	**104.285**	**7.563**	**28.409**
30	**9.931**	**9.931**	**4.016**	**3.178**	**2.568**	**2.911**	**4.154**	**4.154**	**303.674**	**8.045**	**29.377**
32	**10.168**	**10.168**	**4.127**	**3.227**	**2.617**	**2.985**	**4.275**	**4.275**	**155.438**	**8.129**	**30.563**
34	**10.456**	**10.456**	**4.187**	**3.331**	**2.684**	**3.059**	**4.303**	**4.303**	**262.382**	**7.539**	**31.478**

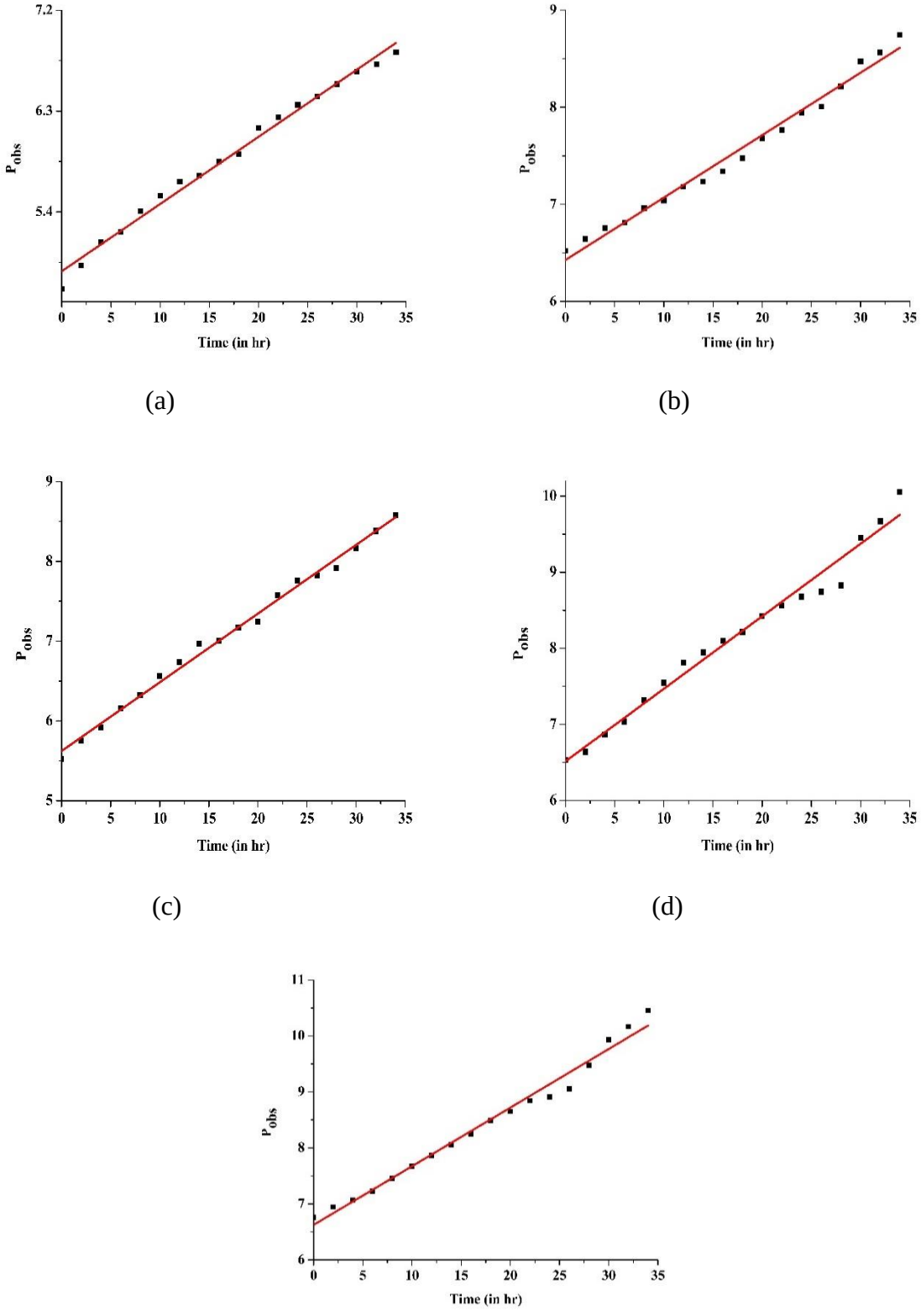

Figure 6: Graph for oscillator strength vs. time (in hrs) for 3H4 →3P2 transition for Praseodymium (III): L-Aspartic acid complex in DMF solvent at various temperatures 25°C, 30°C, 35°C, 40°C and 45°C

Table 9: Rate Constants of Praseodymium (III): L-Aspartic acid complex in DMF solvent

Temp 'K'	1/T x 10^3	Rate Constant 'k' (Mol $L^{-1}hr^{-1}$)	Rate Constant 'k' Mol $L^{-1}s^{-1}$	Log k	Pre-exponential factor 'A'	Activation Energy 'Ea' (kJ)
298	3.3557	0.05997	16.65833	1.22163	16.81879	0.02382
303	3.3003	0.06430	17.86111	1.25191	18.03067	
308	3.2468	0.08619	23.94167	1.37915	24.16578	
313	3.1949	0.09529	26.46944	1.42275	26.71235	
318	3.1447	0.10476	29.10000	1.46389	29.36339	

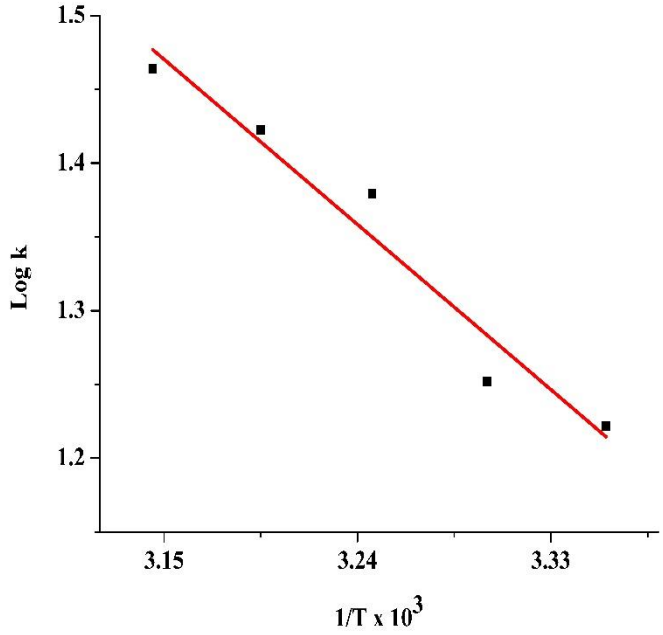

Figure 7: Plot of Log k versus 1/T × 103 for Praseodymium (III): L-Aspartic acid complex in DMF at different temperatures

Table 10: Thermodynamic parameters, activation energy and rate constants for Praseodymium(III):L-Aspartic acid complex

Temperature 'K'	Rate Constant 'k' Mol $L^{-1}s^{-1}$	ΔH (kJ)	ΔG (kJ)	ΔS (kJ)	Activation Energy 'Ea' (kJ)
298	16.65833	0.02382	-6.97044	0.02347	0.02382
303	17.86111		-7.38291	0.02405	
308	23.94167		-8.00126	0.02649	
313	26.46944		-8.52662	0.02732	
318	29.10000		-8.91332	0.02810	

Results and discussion

Hypersensitive transitions are those transitions that obeyed the selection principle |ΔS|=0; |ΔL|≤2; |ΔJ|≤2 and are extremely responsive to fluctuations in the coordination environment [27]. The transitions 3H4→3P2, 3P1, 3P0, and 1D2 of

Praseodymium(III) are non-hypersensitive because they do not obey selection principles. They however have shown significant sensitivity to minute changes in the coordination surroundings of Praseodymium(III). Hence, these non-hypersensitive transitions were named Pseudohypersensitive, and such findings were termed 'Ligand Mediated Pseudohypersensitivity'[28,29]. Absorption spectrophotometry is an extremely useful tool for lanthanide coordination chemistry, especially in solution and non-aqueous media, because most lanthanides have detailed internal f-electron transition spectra in the visible spectral region and are sensitive to the metal-ligand coordination environment. Pr(III) has a paramagnetic property. In the visible region, it has 4f–4f transition spectra (3H4→3P2, 3H4→3P1, 3H4→3P0, &3H4→1D2)[33]. In Pr(III):L-Aspartic acid complex, the intensity of the spectral bands increases dramatically, which could be owing to the ligand involvement in the complexation with Pr (III).

Table 1 shows the comparison of energy interaction parameters: Slater-Condon Fk (cm-1), Lande ξ4f (cm-1), Racah energy Ek (cm-1), nephelauxetic ratio (β), bonding (b1/2) and covalency (δ) factor for Pr(III) and Pr(III):L-Aspartic acid complex in different aquated MeOH, MeCN, DMF and dioxane solvents. When compared to the free Pr(III) state, the values of energy interaction parameters such as Fk, Ek, and ξ4f for Pr(III):L-Aspartic acid complex decreases, indicating a decrease in interelectronic repulsion and spin-orbit interaction parameters, resulting in a decrease in the metal-ligand bond distance, making complexation possible. The decrease in the values of Fk parameters indicates that ligand affects electrostatic repulsion more than spin-orbit coupling. The order of Slater-Condon parameters is found to be F2>F4>F6. According to the nephelauxetic effect, the metal-ligand bond distance must decrease when complexation occurs and its impact depends on the coordination number, according to Jorgensen and Ryan[32]. According to Frey and Dew Horrocks [37], the nephelauxetic effect is connected to the covalency of the metal-ligand bond and the coordination number: the smaller the coordination number, the greater the amplitude of the nephelauxetic effect. In all systems, the nephelauxetic effect is between 0.944-0.948, showing the validity of the study; the positive value of δ could indicate the possibility of a covalent bond formed between the Pr (III) and L-Aspartic acid complex. When complexation occurs between Pr(III) and the L-Aspartic acid, the values of nephelauxetic effect, bonding parameters and covalency factor increase, resulting in the decrease of effective nuclear charge and the interelectronic repulsion parameters. Due to the nephelauxetic effect, the metal-ligand distance is lowered, implying orbital overlapping is more likely to occur, which is a requirement for improving covalency. The binding parameter, often known as the mixing coefficient, is related to β. It is commonly used to assess the extent of engagement of the metal ligands in binding[33]. In Pr(III) spectra, all three of these parameters (β, δ, and b1/2) are utilized to define the degree of covalency. The presence of covalent nature in the metal-ligand bonding is indicated by the positive values of b1/2. Because of the tiny value of b1/2 and the minor change in its values, 4f orbitals are only minimally involved in ligand binding. Sinha's parameter (δ) is usually taken as a measure of covalency.

In table 2 except for the 3H4→1D2 transition, the observed value of energies for 3H4→3P2, 3P1 and 3P0 transitions of Pr (III) and Pr(III):L-Aspartic acid complex are more significant than the calculated value of energies. The precision of different energy interaction parameters: Slater-Condon (Fk), Lande factor (ξ4f), Racah energy (Ek), Nephelauxetic ratio (β), bonding (b1/2) and covalency (δ) factors, is shown by the root mean square deviation (RMS) values.

Table 3 gives the values of oscillator strength (P) and Judd-Ofelt parameters ($T\lambda$) for Praseodymium(III) and Praseodymium(III):L-Aspartic acid complex under various experimental conditions. The table shows that when Pr(III) was added to L-Aspartic acid there were significant changes in the oscillator strength and Judd Ofelt parameters values, which validates the possibility of binding of L-Aspartic acid to Praseodymium(III) in the solution. T2 is not considered since it is associated to the 3H4→3F3 transition, which is beyond the UV-Visible area and has negative findings. Minor changes in the coordinating environment, on the other hand, had a considerable impact on the values of T4 and T6 parameters, which were both positive. Variation in the symmetry characteristics of the complex is connected to both $T4$ and $T6$ parameters[34]; therefore the significant changes in the values of $T4$ and $T6$ suggest changes in the symmetry of Pr(III), its complex systems and their immediate coordination environment. Outer-sphere coordination occurs between the ligand and metal ion when there are small variations in the values of oscillator strength and Judd Ofelt parameters, while inner-sphere coordination occurs when there are large variations in P and Tλ (λ=2,4,6). The change in computed values of P and $T\lambda$ presented in table 3 could provide strong evidence of the involvement of inner-sphere coordination between L-Aspartic acid and Praseodymium (III).

From fig. 3, the absorption bands of Pr (III) complexes shift significantly as compared to Pr (III), demonstrating their sensitivity to small changes in the coordination ambience which induce a wavelength shift towards longer wavelengths, resulting in a redshift and strengthening of the 4f-4f transition spectral bands. A red shift is observed leading to the phenomena of the nephelauxetic effect. The nephelauxetic effect causes the metal-ligand bond length to shorten, leading to the intensification of the 4f-4f bands, indicating the likelihood of ligand binding to the metal ion. Figure 4 shows the comparative spectra of Pr(III) and Pr(III): amino acid complexes in aquated MeOH, MeCN, dioxane and DMF solvents. Variation of solvents brings a significant effect on the oscillator strengths of the 4f-4f bands and consequently marked variation in the magnitudes of intensity Tλ parameters (λ=2,4,6). DMF has high polarizability and sensitivity, which means it efficiently enhances 4f-4f electric dipole intensity and hence could show the possibility of highest covalency for the complexation of Pr(III): Ligands among the four

solvents followed by the solvents MeCN, Dioxane and MeOH.

In particular, ligand properties including ion formation, donor atoms, sizes, and solvation effects influence the coordination numbers and geometries. The coordination number of lanthanides in an aqueous solution is 9 and 8, but it can increase to 12 when a ligand is added [35]. Because of the chelate effect, when praseodymium ions create a complex with ligands that are chelated, the resulting complexes are stronger than when they form a complex with monodentate ligands [36]. When the isoelectric point of an amino acid is preserved, the amino acid exists in solution in its zwitterion form. Amino acids are hard donors, whereas the ionic compound Pr(III) is a hard acceptor. L-Aspartic acid produces zwitterion at pH 2.98 in an aqueous solution because at this pH, Pr(III) and the amino acid's oxygen atom form complex [23–25]. The oxygen donor of L-aspartic acid and the praseodymium ion created a stable complex with a 9-coordination number. For the nona-coordinated Pr(III):L-Aspartic acid combination in an aqueous media, Figure 2 depicts potential chemical reaction routes.

Five sets of kinetic experiments were analysed at various temperatures (298K, 303K, 308K, 313K, and 318K) to indicate changes in the value of absorbance over time. The kinetic studies were executed by examining the rising variations in absorbance with time corresponding to four bands in the complexation of Praseodymium(III) with L-Aspartic acid, as illustrated in Figure 5 all four bands of the Pr(III): L-Aspartic acid complex are equally sensitive. The rate constants were calculated by plotting oscillator strength over time in Figure 6 and listing them in Tables 4-8; oscillator strength graphs develop linearly with time. The absorbance and oscillator strength of the various absorption transition bands can thus be used to explore the Pr (III) and L-Aspartic acid complexation reaction pathways. Absorption spectrum analysis can be used to investigate the kinetics of Pr (III) complexation with L-Aspartic acid since the strength of 4f- 4f transitions increases over time. Table 9 shows the measured rates (k) in terms of the complex formed during the reaction, as well as plots of oscillator intensity of $3H4 \rightarrow 3P2$ transitions for Pr(III):L-Aspartic acid complex vs. time. We can see from the table that when the temperature rises, the rate constant values of complexation rise as well, which is consistent with the Arrhenius equation's theoretical prediction. Additionally, when the temperature rises, the values of the Pre-exponential factor (A) rise, increasing the probability of molecules collision. The Van't Hoff equation is used to compute the activation energy (Ea) and other thermodynamic parameters (ΔGo, ΔHo and ΔSo); figure 7 depicts a plot of 1/T against ln k. The rate of complexation has been conclusively proved to increase with increasing temperature, and this is used to compute the activation energy Ea of the complexation. Table 10 shows that the values of the thermodynamic parameters ΔHo and ΔSo are positive, indicating that the complexation reaction is endothermic and that entropy is increasing. In addition, because $T\Delta So > \Delta Ho$, the coordinating reaction is entropy-driven. Negative ΔGo values imply that complex formation is favoured and spontaneous, as shown in all of Pr(III) and L-Aspartic acid complex systems. As a result, we can further justify that as the system approaches higher temperatures (increasing ΔSo values), the complexation process between Pr(III) and L-Aspartic acid takes place at a random pace. The activation energy (Ea) for the complexation of Pr(III) with L-Aspartic acid in DMF solvent was found to be 0.02382 kJ, lower values of Ea substantiate recent information about the reaction's spontaneity.

Conclusion

For Praseodymium(III) complexes, a drop in the Lande factor, Racah energy, and Slater-Condon parameters points to a reduction in interelectronic repulsion and spin-orbit interaction, which in turn causes a reduction in the metal-ligand bond distance. The nephelauxetic effect is found to be between 0.944-0.948, showing the validity of the study and indicating the possibility of a covalent bond formed between the Pr (III) and L-Aspartic acid complex. The increased values of the Nephelauxetic ratio, bonding parameters and covalency factor as well as the resulting decrease of effective nuclear charge and the interelectronic repulsion parameters signify the formation of complex Pr(III):L-Aspartic acid. The appearance of redshift is caused by the intensification of the absorption bands that arise from complexation between Pr (III) and L-Aspartic acid. A red shift is observed leading to the phenomena of the nephelauxetic effect. The nephelauxetic effect causes the metal-ligand bond length to shorten, leading to the intensification of the 4f-4f bands, indicating the possibility of ligand binding to the metal ion. The ligand, L-Aspartic acid's role in the inner-sphere coordination of Pr (III) may be strongly supported by the fluctuations in the estimated values of P and Tλ. With the oxygen donor ligands of L-aspartic acid, praseodymium ions form a stable complex, and the inner sphere coordination produces a nona-coordination number. The considerable variations in $T4$ and $T6$ readings show that the symmetry has changed. DMF has high polarizability and sensitivity, which means it efficiently enhances 4f-4f electric dipole intensity and hence could show the possibility of highest covalency for the complexation of Praseodymium (III): Ligands among the four solvents followed by the solvents MeCN, Dioxane and MeOH. The 4f-4f band intensities of the organic solvents have sensitivity in the order:

$$DMF > CH3CN > C4H8O2 > CH3OH$$

It reveals that the changing oscillator strengths of different 4f-4f transitions over time could aid in determining the nature of the reaction pathways for the complexation of L-Aspartic acid with Pr(III) in DMF solvent. The rate of complexation increases

with time and temperature confirming the Arrhenius prediction of the reaction rate. The positive values of ΔHo and ΔSo indicate that the complexation reaction is endothermic and that entropy is increasing. Furthermore, negative ΔGo values indicate a favourable and spontaneous complex formation. The rate of the reaction for Pr(III):L-Aspartic acid complex increases with temperature and the activation energy are found to be 0.02382 KJ, the lower values of Ea substantiate information on the reaction's spontaneity. The empirical relation between temperature and reaction rate is provided by the readings of the pre-exponential factor (A), which is dependent on the possibility of how often the molecules collide.

Acknowledgement

The authors wish to acknowledge the Department of Chemistry, Nagaland University, Lumami, India for providing the laboratory facilities. The authors are grateful to UGC NON-NET fellowship, India for their financial support.

REFERENCES

[1] A.J. Amoroso, S.J.A. Pope, Using lanthanide ions in molecular bioimaging, Chem. Soc. Rev. 44 (2015) 4723–4742. https://doi.org/10.1039/C4CS00293H.
[2] S. Procházková, J. Hraníček, V. Kubíček, P. Hermann, Formation kinetics of europium(III) complexes of DOTA and its bis(phosphonate) bearing analogs, Polyhedron. 111 (2016) 143–149. https://doi.org/10.1016/J.POLY.2016.03.039.
[3] J.A. Cotruvo, The Chemistry of Lanthanides in Biology: Recent Discoveries, Emerging Principles, and Technological Applications, ACS Cent. Sci. (2019). https://doi.org/10.1021/acscentsci.9b00642.
[4] S. Philip, P.S. Thomas, K. Mohanan, Synthesis, fluorescent studies, antioxidative and α-amylase inhibitory activity evaluation of some lanthanide(III) complexes, J. Serbian Chem. Soc. 83 (2018) 561–574. https://doi.org/10.2298/JSC180918010P.
[5] Y. Zhang, W. Thor, K.L. Wong, P.A. Tanner, Determination of Triplet State Energy and the Absorption Spectrum for a Lanthanide Complex, J. Phys. Chem. C. 125 (2021) 7022–7033. https://doi.org/10.1021/ACS.JPCC.1C00158/SUPPL_FILE/JP1C00158_SI_001.PDF.
[6] M.N. Gueye, M. Dieng, I.E. Thiam, D. Lo, A.H. Barry, M. Gaye, P. Retailleau, Lanthanide(III) complexes with tridentate Schiff base ligand, antioxidant activity and X-ray crystal structures of the Nd(III) and Sm(III) complexes, South African J. Chem. 70 (2017) 08–15. https://doi.org/10.17159/0379-4350/2017/V70A2.
[7] H. Li, X. Wang, D. Huang, G. Chen, Recent advances of lanthanide-doped upconversion nanoparticles for biological applications, Nanotechnology. (2020). https://doi.org/10.1088/1361-6528/ab4f36.
[8] S.N. Misra, M.A. Gagnani, D.M. Indira, R.S. Shukla, Biological and Clinical Aspects of LanthanideCoordination Compounds, Bioinorg. Chem. Appl. 2 (2004) 155. https://doi.org/10.1155/S1565363304000111.
[9] N. Bendangsenla, T. Moainla, J. Sanchu, M.I. Devi, N. Bendangsenla, T. Moainla, J. Sanchu, M.I. Devi, Computation of Energy, Intensity and Thermodynamic Parameters for the Interaction of Ln(III) with Nucleic Acid: Analysis of Structural Conformations, Chemical Kinetics and Thermodynamic Behaviour through 4f-4f Transition Spectra as Probe, J. Mater. Sci. Chem. Eng. 6 (2018) 169–183. https://doi.org/10.4236/MSCE.2018.67018.
[10] M. Ziekhrü, Z. Thakro, C. Imsong, J. Sanchu, M. Indira Devi, Computation of energy interaction and intensity parameters for the complexation of Pr(III) with glutathione at different pH in the presence/absence of Mg2+: 4f-4f transition spectra as a probe, Polyhedron. 200 (2021) 115099. https://doi.org/10.1016/J.POLY.2021.115099.
[11] T. Maruyama, Y. Fujimoto, T. Maekawa, Synthesis of gold nanoparticles using various amino acids, J. Colloid Interface Sci. 447 (2015) 254–257. https://doi.org/10.1016/J.JCIS.2014.12.046.
[12] K.K. Gangu, S. Maddila, S.N. Maddila, S.B. Jonnalagadda, Nanostructured Samarium Doped Fluorapatites and Their Catalytic Activity towards Synthesis of 1,2,4-Triazoles., Molecules. 21 (2016). https://doi.org/10.3390/MOLECULES21101281.
[13] S. Shankar, J.W. Rhim, Amino acid mediated synthesis of silver nanoparticles and preparation of antimicrobial agar/silver nanoparticles composite films, Carbohydr. Polym. 130 (2015) 353–363. https://doi.org/10.1016/J.CARBPOL.2015.05.018.
[14] C.H. Evans, C.H. Evans, The Interaction of Lanthanides with Amino Acids and Proteins, in: Biochem. Lanthanides, 1990. https://doi.org/10.1007/978-1-4684-8748-0_4.
[15] N. Ranjana Devi, H. Bimola, C. Sumitra, N. Rajmuhon Singh, Energy and electric dipole intensity parameters for the 4f-4f transitions for the complexation of Pr III and Nd III with dicyandiamide in different solvents in presence and absence of Ca II to explore the similarities between Ln III and Ca II, J. Indian Chem. Soc. (2012).
[16] C. Victory Devi, N. Rajmuhon Singh, Spectrophotometric study of kinetics and associated thermodynamics for the complexation of Pr(III) with l-proline in presence of Zn(II), Arab. J. Chem. 10 (2017) S2124–S2131. https://doi.org/10.1016/J.ARABJC.2013.07.044.
[17] R.S. Naorem, N.P. Singh, N.M. Singh, 4f–4f Spectral Analysis and Solvent Effect for the Interaction of Pr(III) with l-Tryptophan Using Different Aquated Solvents in the Presence and Absence of Zn(II), Chem. Africa 2019 31. 3 (2019) 171–180. https://doi.org/10.1007/S42250-019-00111-9.
[18] N. Bendangsenla, T. Moainla, J. Sanchu, M.I. Devi, N. Bendangsenla, T. Moainla, J. Sanchu, M.I. Devi, Computation of Energy, Intensity and Thermodynamic Parameters for the Interaction of Ln(III) with Nucleic Acid: Analysis of Structural Conformations, Chemical Kinetics and Thermodynamic Behaviour through 4f-4f Transition Spectra as Probe, J. Mater. Sci. Chem. Eng. 6 (2018) 169–183. https://doi.org/10.4236/MSCE.2018.67018.
[19] T. Moaienla, N. Bendangsenla, M.I. Devi, A Probe into the Kinetics of the Interaction of Pr(III) Ions with Some Selected Amino Acids: A 4f-4f Transition Spectral Study, Adv. Mater. Sci. Appl. 3 (2014) 157–163. https://doi.org/10.5963/AMSA0303007.
[20] Y. Hasegawa, Y. Kitagawa, T. Nakanishi, Effective photosensitized, electrosensitized, and mechanosensitized luminescence of lanthanide complexes, NPG Asia Mater. 2018 104. 10 (2018) 52–70. https://doi.org/10.1038/s41427-018-0012-y.
[21] A. Carac, R. Boscencu, G. Carac, S.G. Bungau, Spectral study of some lanthanides complexes with quaternary pyridinium ligands, Rev. Chim. 68 (2017) 2265–2269. https://doi.org/10.37358/RC.17.10.5868.
[22] M. Remko, D. Fitz, R. Broer, B.M. Rode, Effect of metal Ions (Ni 2+, Cu 2+ and Zn 2+) and water coordination on the structure of L-phenylalanine, L-tyrosine, L-tryptophan and their zwitterionic forms, J. Mol. Model. 17 (2011) 3117–3128. https://doi.org/10.1007/S00894-011-1000-0/TABLES/6.
[23] F. Costanzo, R.G. Della Valle, V. Barone, MD simulation of the Na+-phenylalanine complex in water: competition between cation-pi interaction and

aqueous solvation, J. Phys. Chem. B. 109 (2005) 23016–23023. https://doi.org/10.1021/JP055271G.
[24] A.L. Sobolewski, D. Shemesh, W. Domcke, Computational studies of the photophysics of neutral and zwitterionic amino acids in an aqueous environment: Tyrosine-(H2O)2 and tryptophan-(H2O)2 clusters, J. Phys. Chem. A. 113 (2009) 542–550. https://doi.org/10.1021/JP8091754/SUPPL_FILE/JP8091754_SI_001.PDF.
[25] J.C.G. Bünzli, C. Piguet, Lanthanide-containing molecular and supramolecular polymetallic functional assemblies, Chem. Rev. 102 (2002) 1897–1928. https://doi.org/10.1021/CR010299J/ASSET/CR010299J.FP.PNG_V03.
[26] W.T. Carnall, P.R. Fields, B.G. Wybourne, Spectral Intensities of the Trivalent Lanthanides and Actinides in Solution. I. Pr3+, Nd3+, Er3+, Tm3+, and Yb3+, J. Chem. Phys. 42 (2004) 3797. https://doi.org/10.1063/1.1695840.
[27] R.D. Peacock, Hypersensitivity of spectral bands in complexes of praesodymium(III), Chem. Phys. Lett. (1970). https://doi.org/10.1016/0009-2614(70)80282-2.
[28] S.N. Misra, S.O. Sommerer, The ligand mediated pseudohypersensitivity of the 3H4 → 3P2, 3H4 → 3P1, 3H4 → 3P0, and 3H4 → 1D2 transitions of praseodymium(III) complexes in solution media, Https://Doi.Org/10.1139/V92-009. 70 (2011) 46–54. https://doi.org/10.1139/V92-009.
[29] S.N. Misra, K. John, Difference and Comparative Absorption Spectra and Ligand Mediated Pseudohypersensitivity for 4f-4f Transitions of Pr(lll) and Nd(lll), Http://Dx.Doi.Org/10.1080/05704929308018115. 28 (2006) 285–325. https://doi.org/10.1080/05704929308018115.
[30] W.T. Carnall, P.R. Fields, B.G. Wybourne, Spectral Intensities of the Trivalent Lanthanides and Actinides in Solution. I. Pr3+, Nd3+, Er3+, Tm3+, and Yb3+, J. Chem. Phys. 42 (2004) 3797. https://doi.org/10.1063/1.1695840.
[31] E.Y. Wong, Configuration interaction of the Pr3+ ion, J. Chem. Phys. (1963). https://doi.org/10.1063/1.1733794.
[32] C. Klixbüll Jørgensen, R. Pappalardo, H.H. Schmidtke, Do the ``Ligand Field'' Parameters in Lanthanides Represent Weak Covalent Bonding?, J. Chem. Phys. 39 (2004) 1422. https://doi.org/10.1063/1.1734458.
[33] R.B. Martin, F.S. Richardson, Lanthanides as probes for calcium in biological systems, Q. Rev. Biophys. 12 (1979) 181–209. https://doi.org/10.1017/S0033583500002754.
[34] J. Sanchu, M. Ziekhrü, Z. Thakro, M.I. Devi, 4f-4f Transition Spectra of the Interaction of Pr(III) with L-Valine in Solution: Kinetics and Thermodynamic Studies, Asian J. Chem. 34 (2022) 2688–2696. https://doi.org/10.14233/AJCHEM.2022.23911.
[35] A.A. Khan, H.A. Hussain, K. Iftikhar, 4f-4f absorption spectra and hypersensitivity in nine-coordinate Ho(III) and Er(III) complexes in different environments., Spectrochim. Acta. A. Mol. Biomol. Spectrosc. 60 (2004) 2087–2092. https://doi.org/10.1016/J.SAA.2003.10.042.
[36] S.P. Sinha, Structure and bonding in highly coordinated Lanthanide complexes, (1977) 69–149. https://doi.org/10.1007/3-540-07508-9_3.
. Ars Pharm. 2016;57(2):77–87.